Low Temperature Physics/Fizika Nizkikh Temperatur, 2012, v. 38, No. 11, pp. 1300–1305

Mutual interactions between objects oscillating in isotopically pure superfluid ^{4}He in the $T \to 0$ limit

D. Garg[1], V.B. Efimov[1,2], M. Giltrow[1], P.V.E. McClintock[1], and L. Skrbek[3]

[1]*Department of Physics, Lancaster University, Lancaster, LA1 4YB, UK*

[2]*Institute of Solid State Physics RAS, Chernogolovka 142432, Moscow Region, Russia*
E-mail: efimov@issp.ac.ru

[3]*Faculty of Mathematics and Physics, Charles University, Ke Karlovu 3, Prague 121 16, Czech Republic*

Received June 13, 2012

We report the results of experiments to explore interactions between physically separated oscillating objects in isotopically pure superfluid ^{4}He at $T \sim 10$ mK. The investigations focused mainly on 32 kHz quartz tuning forks, but also consider a nearby 1 kHz oscillating grid. The low-drive linewidth (LDL) and resonant frequency f_d of a detector fork were monitored while the maximum velocity of a transmitter fork, separated from the detector by a few mm, was varied over a wide range. Clear evidence was found for mutual interactions between the two forks, and for the influence of the grid on the forks. Monitoring the detector's LDL and f_d provides evidence for a generator critical velocity in the range $0.3 < v_{c1} < 1.0$ cm/s for onset of the detector responses, in addition to a second critical velocity $v_{c2} \sim 13$ cm/s probably corresponding to the production of quantum turbulence at the generator. The results are discussed, but are not yet fully understood.

PACS: *67.25.dk* Vortices and turbulence;
47.27.Cn Transition to turbulence.

Keywords: superfluid helium, tuning fork, oscillating grid, quantum turbulence, acoustic resonance.

In Celebration of Professor Leonid P. Mezhov-Deglin's 75th Birthday

1. Introduction

First, we are much indebted to the Editorial Board of *Low Temperature Physics* for their invitation to contribute to this special issue marking the 75th birthday of Professor Leonid P. Mezhov-Deglin, whose seminal and imaginative contributions to low temperature physics still continue after spanning more than half a century.

In what follows, we describe an extension of a recent investigation [1] of individual quartz tuning forks oscillating in isotopically pure superfluid ^{4}He near 10 mK. We report the results of experiments to measure the mutual interactions between pairs of forks, and to study the influence on individual forks of quantum turbulence (QT) being generated by a nearby oscillating grid.

Quantum turbulence is currently being investigated through studies of the resonant dynamics of a variety of different objects oscillating in both He II and ^{3}He–B, attracting considerable attention and interest. Examples of such objects include spheres [2–4], wires [5–10] and grids [11–13]. Quartz tuning fork resonators [14–16] are the latest sensors to join this family of vibrating objects. They are quite small ($\sim$ mm), and therefore convenient for use at low temperatures. They have been used as thermometers, viscometers and pressure sensors [15] in all the helium fluids, as well as in QT studies in He II. Forks have been shown [15,17–21] to generate QT over a wide range of temperatures. The question naturally arises, therefore, as to whether forks can also act as detectors of vortex lines? In He II at relatively high temperatures, $T > 1.3$ K, attempts to answer this question suggest that the detection is at best inefficient: a standard 32 kHz fork has been shown to detect a submerged counterflow jet [22], but only if its velocity exceeds about 20 cm/s, and attempts to detect even a rather high vortex line density generated at 1.3 K between counterrotating discs seem not to have been successful [20]. It has been shown, however, that free vortex rings from a fine vibrating wire can trigger the transition to turbulence in the initially vortex-free boundary flow around another vibrating wire at ~ 30 mK [23].

Although superfluid ^{4}He in its low-T limit is much like a vacuum, or æther, interactions between a pair of objects can occur through the creation of excitations that pass from one to the other. In addition to quantized vortices, there may be individual phonons travelling ballistically, or waves of first sound made up of large numbers of coherent phonons; second sound does not exist at these temperatures because there is no normal fluid component *per se*. Rotons are unlikely to be created on account of the relatively large velocities needed [24–26]. So in seeking explanations for any interactions that are observed between uncharged oscillators in the absence of magnetic fields, the only mechanisms needing to be considered are probably those involving either phonons/sound or vortices/QT.

Quantum turbulence is created in the superfluid by an oscillating object when it exceeds a critical velocity $v_{c2} \sim$ ~ 10 cm·s^{-1}. There is also evidence for a lower critical velocity $v_{c1} \sim$ 0.1–0.9 cm·s^{-1} at which there are changes in flow that can lead to increased dissipation. The underlying mechanism is unknown, but some possibilities are discussed in [1].

It has recently become apparent that emission of sound from forks can provide an important source of energy loss [1,27,28], leading to their low-drive-linewidths (LDLs) being much larger than in a vacuum. Calculations [1] have shown that the dissipation at low drives can be attributed to coupling of the oscillatory modes of the fork to acoustic modes of the experimental cell containing the helium sample, considered as a resonant cavity. For a relatively large cell, as used in our present experiments, the acoustic modes are very closely-spaced. Consequently, tiny changes in the velocity of sound, corresponding to very small pressure variations in the cell, can bring them into or out of resonance with the fork, resulting in corresponding variations in the LDL.

2. Experimental techniques

The experiment was performed in a ^{3}He–^{4}He dilution refrigerator at its base temperature of $\sim$ 10 mK. The large experimental cell, holding $\sim 1.5\ell$ of isotopically pure ^{4}He under a pressure of 5 bar, was described earlier in connection with vibrating grid experiments [13,29,30]. The arrangement of the forks and grid in the cell is described in [1]. Briefly, one fork (f_1) was on the cylindrical axis of the cell, 1 mm above the grid. The other one (f_2) was mounted 10 mm above f_1. The forks oscillated in planes parallel with the grid, but were mounted with an angle of 120° between their axes of symmetry. A third fork positioned outside the electrode structure (f_3) was not in line-of-sight of the grid or other forks. Forks f_1 and f_2 were bare, with their encapsulating cans completely removed; the can of f_3 was left in place, but it was opened by removal of its top to allow access by the superfluid helium.

The filling tubes to the cell descended through the main ^{4}He bath at 4.2 K, and were closed off by valves at the top of the cryostat. As the level of helium gradually fell in the bath, the pressure rose by about 0.02 bar, causing the velocity of sound to increase by about 4 parts in 10^4 which (see Sec. 1) was sufficient to cause one or more acoustic modes to pass through resonance with the fork oscillations. Consequently, although results are highly reproducible over a few tens of minutes, measurements of the LDL or resonant frequency on longer timescales were typically characterised by slow oscillatory drifts. The latter must be borne in mind thoughout the rest of the paper but, because we are mostly looking for responses to changes, they do not in general have a large influence on the interpretation of the results.

3. Experimental results

To seek evidence of inter-fork interactions, we operated f_1 as a detector and f_2 as a generator. In what follows, the numbers given for both the generator and detector responses corresponds to the maximum prong velocity in each case.

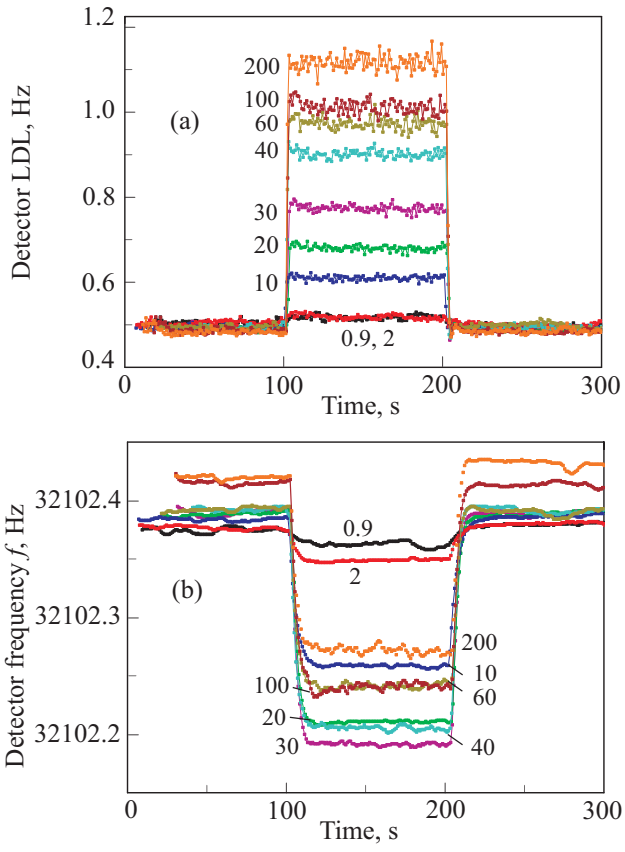

Fig. 1. Response of the detector fork f_1 to switching on the excitation of the generator f_2. The low-drive linewidth Δf_d (a) and frequency f (b) are plotted as functions of time for the generator velocities indicated by the numbers (in mV_{RMS}) beside the traces. The generator is switched on at $t = 100$ s, and off at $t = 200$ s. The detector velocity was 0.3 mm/s, i.e., $v < v_{c_1}$.

Calculations of the prong velocity, and of the force on the fork due to the excitation, were based on the relationships given by Blaauwgeers *et al*. [15]. In our experiments at $T \sim 10$ mK a slow change in the behaviour of the fork response $v_{\max}(F) \propto F$ began at a velocity $v_{\max} \sim 1$ cm/s [1]. A transition to QT generation by the fork began at the the much higher velocity of ~ 15 cm/s, where it manifested as a dependence $v_{\max}(F) \propto F^2$. The detector was continuously driven at a low level ($v \sim$ 0.3 mm/s), and its LDL and resonant frequency were monitored. Figure 1 shows how the detector responds when the generator is driven on resonance for periods of 100 s, each successive period corresponding to an increased generator drive. For generator velocities that are less than a certain value, probably corresponding to v_{c1} (see Sec. 1), there is almost no effect. At higher generator velocities the LDL of the detector increases linearly (not illustrated), and the detector frequency falls, until the generator velocity reaches a critical value probably corresponding to v_{c2}. Above this second critical velocity the LDL of the detector continues to increase, albeit at a slower rate, while the detector frequency starts to increase again. In some experiments the detector response was more complicated. For example, the change of behaviour of the LDL on exceeding v_{c2} may manifest either as an increasing LDL or to a decreasing LDL, as we discuss below.

We have also conducted experiments in which the detector LDL and resonant frequency were tracked continuously, but where the velocity of the generator was steadily and slowly ramped up and then down, without switching it off, with results as shown in Fig. 2(a)–(c). It is clear that the detector LDL (b) does not start to change noticeably until the generator velocity (a) has attained a value that is of order $v_{c1} \sim$ 1 cm/s, whereupon it increases rapidly until the generator velocity has reached a value of order $v_{c2} \sim$ 13 cm/s, after which it starts decreasing again. The behavior is nicely mirrored as the generator velocity ramps down again. A similar measurement conducted with a much higher detector velocity ($\sim$ 40 cm/s, within the turbulent regime) showed only a negligible detector response to the generator.

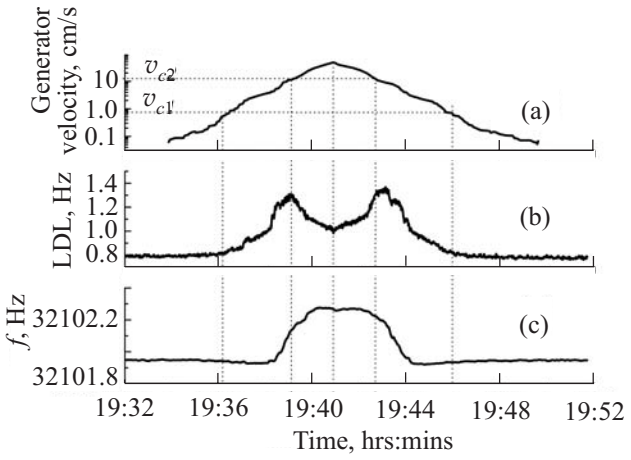

Fig. 2. Generator f_2 velocity and corresponding detector f_1 responses while the generator drive amplitude is swept continuously up and then down again. Resultant generator velocity (a). Resonant width (b) and resonant frequency of the detector (c). The detector velocity was 0.3 mm/s, i.e., $v < v_{c_1}$.

We note that the results shown in Figs. 1 and 2(a)–(c) are qualitatively different, in that the detector LDL increases monotonically with increasing generator drive in the former case, while in the latter case the detector LDL falls when the generator velocity exceeds v_{c2}. This difference seems not to be due to the different experimental procedure, but rather to a non-reproducibility of the detector response. This is confirmed in the data of Fig. 3 where, in effect, the measurements of Fig. 2 were repeated four times at intervals during a 4-hour period. The results at about 14:50, for example, were rather similar to those of Fig. 2; in those near 13:15 the LDL variation was opposite in sign, but the positive monotonic change in resonant frequency was similar to that seen in Fig. 2(b). If the roles of the detector and the generator forks were exchanged, qualitatively very similar behaviour was observed. Comparable interactions with f_3 could also be detected but were much weaker.

Evidence was found for the influence of the grid on forks f_1 and f_2, but there was no measurable influence of either fork on the grid. Figure 4 illustrates the changes in the LDL and resonant frequency of f_1 while the amplitude of the driving force on the grid is slowly ramped up and then ramped down again. The velocity of the grid, plotted in (a) is flat-topped on account of QT production once v_2 has been exceeded. Panels (b) and (c) show clear evidence for almost discontinuous changes in Δf and f when the grid velocity is near v_2, but they are extremely small.

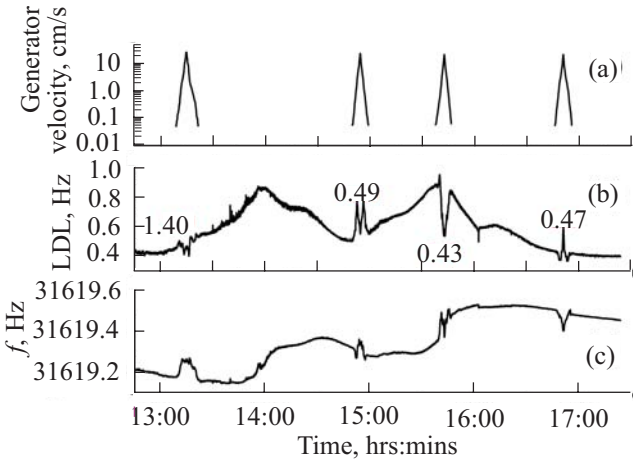

Fig. 3. Four episodes in which the generator f_2 drive amplitude is swept continuously up and then down again, much as in Fig. 2. Resultant generator velocity (a), resonant width (b) and resonant frequency of the detector f_1 (c). The detector velocity was 0.3 mm/s, i.e., $v < v_{c_1}$. The corresponding generator LDLs are shown by the numbers adjacent to the responses.

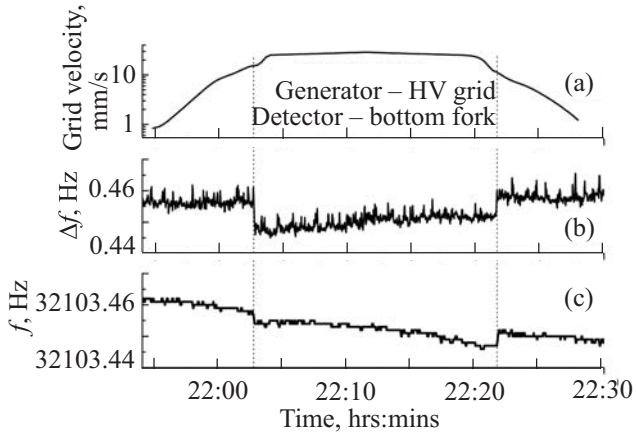

Fig. 4. Observation of grid-to-fork influence, showing the grid velocity and corresponding detector responses while the grid drive amplitude is swept continuously up and then down again. The detector velocity was 0.3 mm/s, i.e., $v < v_{c_1}$. Resultant grid velocity (a), resonant width (b) and resonant frequency of the detector fork f_1 (c).

Note that the "tilt" on both plots is attributable to the tiny pressure changes discussed in Sec. 2.

Figure 5 illustrates the influence of the grid on f_2, over a longer interval: in effect, it shows 4 repeats of Fig. 4, but using f_2, and with the grid quiescent for most of the time. As shown in (a) the grid velocity is swept up and down slowly, 4 times. The resultant changes in Δf and f are plotted in (b) and (c), respectively. Nearly discontinuous changes occur in both quantities, superimposed on slowly drifting backgrounds. Of particular note is the fact that the changes in Δf and f in response to the grid being energised can be either positive or negative.

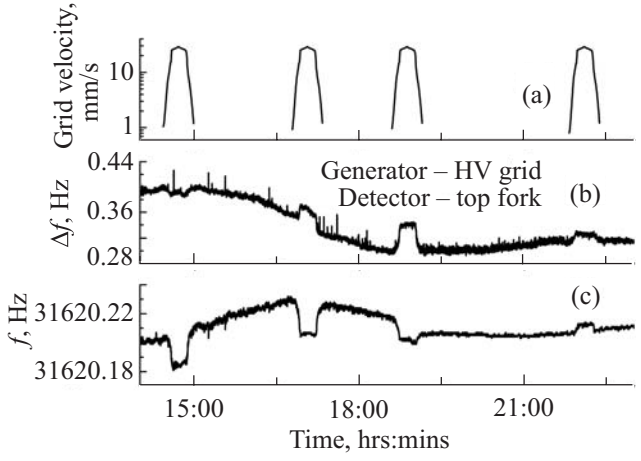

Fig. 5. Four episodes in which the grid drive amplitude is swept continuously up and then down again, much as in Fig. 4; in between these episodes the grid was undriven. Grid velocity, (a), resonant width (b) and resonant frequency of the detector fork f_2 (c). The detector velocity was 0.3 mm/s, i.e., $v < v_{c_1}$.

4. Discussion and conclusions

It is clearly evident from the experimental results that the forks and grid affect each other, but that their mutual influence is complex. We emphasize that the coupling definitely occurs via the superfluid: the detector does not respond to the generator in vacuum, and nor does it do so in He I. The resonant frequencies (32.102 kHz and 31.615 kHz for forks f_2 and f_1, respectively) are sufficiently far apart that the possibility of electrical cross-talk can be ignored, as can also a possible resonant response of the detector to mechanical vibrations of the generator. The same is true *a fortiori* for a fork and the grid. The fork velocities are many orders of magnitude below those needed for direct roton or phonon generation.

As mentioned above, acoustic coupling of the forks to cavity modes is always important, and the slow time-variations can be attributed to this effect, but it is not clear whether or how it would affect inter-fork coupling. The onset of communication near the generator v_{c1} and the sudden change in behaviour at its v_{c2} would not be expected for a gradually increasing acoustic field. So it seems likely that quantized vortices are involved, especially in the latter case.

The results of Fig. 2 show that the onset of the increase in LDL occurs at $\sim v_{c1}$, and the subsequent sudden decrease in LDL occurs at $\sim v_{c2}$. Figure 5 shows, however, that the response of the detector fork can be exactly opposite in sign: the initial interaction as the generator velocity increases can be either positive or negative, but still with a sign-reversal above the second critical velocity. These variations in the sign of the detector response, as exemplified in Figs. 3 and 5, are puzzling. It seems, however that, at least for the relatively small number of data recorded, the detector LDL at the time of the measurement may be significant. In Fig. 3(b), for example, the sign of the LDL changes depends on whether the initial LDL is above or below 0.5 Hz. For lower LDL, the initial response at $\sim v_{c1}$ is always negative, but the LDL starts to increase again at $\sim v_{c2}$. For initial LDLs above 0.5 Hz, exactly the opposite behavior is seen. In the case of the LDL in grid-fork interactions (Fig. 5(b)) the initial response is negative if the initial LDL is above 0.36 Hz, and positive if the initial LDL is below this width. The frequency changes associated with fork-fork or grid-fork interactions do not seem to depend on the initial LDL in any consistent way.

It seems implausible that the grid could produce significant acoustic effects, given its relatively low resonant frequency of $\omega/2\pi \sim 1$ kHz and the fact that acoustic emission from a dipolar source of this kind should be proportional to ω^4. The well-established acoustic effects for forks, on the other hand, are consistent with their higher frequency (here 32 kHz) and the fact that, as quadrupole sources, their emission should vary as ω^6 as discussed in detail by Bradley *et al.* [31]. It is evident from Fig. 4 that,

consistent with the earlier work at higher temperatures [20,22], the influence of QT on a fork is very weak. It also appears oddly discontinuous. The onset of the change in Δf is very sudden, but then it hardly alters although the QT density is increasing very substantially as the driving force on the grid is ramped towards its maximum. In common with the fork-fork interactions, the grid-fork interaction can be either positive or negative (Fig. 5).

Although we have no detailed understanding of the mechanism underlying the sign changes in the responses, it seems very likely to be associated with acoustics, perhaps in combination with vortices. Tiny changes in the frequency mismatch between the fork and an acoustic mode can result in drastic changes in the response (see Fig. 8 of [1]). One may speculate, for example, that the impinging vortices will always tend to load the fork thereby reducing its frequency. Depending on whether the fork frequency is just above or just below the nearest acoustic mode of the cell, the coupling of the fork to the acoustic mode could be either increased or reduced, with a corresponding increase or reduction in Δf; in addition, one might expect the presence of vortices to have some direct influence in increasing Δf. Yet another possible effect to be borne in mind could involve QT shielding the detector fork from a flux of vortex rings from the fork generator when operated in the high velocity range. Which of these effects is dominant could depend on the separation in frequency of the fork oscillation from the acoustic mode.

In summary, therefore, we can conclude that in "free space" within the æther of superfluid ^{4}He in its low temerature limit:

— Tuning forks exhibit measurable interactions, probably attributable to quantized vortices but complicated by the couplings between the forks and acoustic modes of the cell. In particular, we observed marked changes in the detector response characteristics as the generator velocity passed through the velocity v_{c1} and exceeded the critical velocity v_{c2}.

— A tuning fork can detect the oscillations of a nearby grid, probably by being affected by the QT it is generating — but it is relatively insensitive as a QT detector.

— For both fork-fork and grid-fork interactions, the response can be of either sign; but there are indications that the magnitude of the initial detector LDL may be what determines the sign of the LDL changes observed as the generator power is changed.

Further work will be needed to arrive at a detailed understanding of the phenomena discussed above, in particular to try to separate the acoustic and vortex-influenced effects, perhaps through use of a cell with walls or internal components designed to maximise acoustic absorption.

We gratefully acknowledge many valuable discussions with W.F. Vinen. The investigations were supported by the Engineering and Physical Sciences Research Council (UK) and the Russian Academy of Sciences programme "Quantum mesoscopic disordered systems".

1. Deepak Garg, V.B. Efimov, M. Giltrow, P.V.E. McClintock, L. Skrbek, and W.F. Vinen, *Phys. Rev. B* **85**, 144518 (2012).
2. J. Jäger, B. Schuderer, and W. Schoepe, *Phys. Rev. Lett.* **74**, 566 (1995).
3. J. Luzuriaga, *J. Low Temp. Phys.* **108**, 267 (1997).
4. M. Niemetz, H. Kerscher, and W. Schoepe, *J. Low Temp. Phys.* **126**, 287 (2002).
5. H. Yano, A. Handa, H. Nakagawa, K. Obara, O. Ishikawa, T. Hata, and M. Nakagawa, *J. Low Temp. Phys.* **138**, 561 (2005).
6. H. Yano, N. Hashimoto, A. Handa, M. Nakagawa, K. Obara, O. Ishikawa, and T. Hata, *Phys. Rev. B* **75**, 012502 (2007).
7. N. Hashimoto, R. Goto, H. Yano, K. Obara, O. Ishikawa, and T. Hata, *Phys. Rev. B* **76**, 020504 (2007).
8. D.I. Bradley, *Phys. Rev. Lett.* **84**, 1252 (2000).
9. D.I. Bradley, S.N. Fisher, A.M. Guénault, M.R. Lowe, G.R. Pickett, A. Rahm, and R.C.V. Whitehead, *Phys. Rev. Lett.* **93**, 235302 (2004).
10. D.I. Bradley, S.N. Fisher, A.M. Guénault, R.P. Haley, V. Tsepelin, G.R. Pickett, and K.L. Zaki, *J. Low Temp. Phys.* **154**, 97 (2009).
11. H.A. Nichol, L. Skrbek, P.C. Hendry, and P.V.E. McClintock, *Phys. Rev. Lett.* **92**, 244501 (2004).
12. D.I. Bradley, D.O. Clubb, S.N. Fisher, A.M. Guénault, R.P. Haley, C.J. Matthews, G.R. Pickett, V. Tsepelin, and K. Zaki, *Phys. Rev. Lett.* **95**, 035302 (2005).
13. D. Charalambous, L. Skrbek, P.C. Hendry, P.V.E. McClintock, and W.F. Vinen, *Phys. Rev. E* **74**, 036307 (2006).
14. D.O. Clubb, O.V.L. Buu, R.M. Bowley, R. Nyman, and J.R. Owers–Bradley, *J. Low Temp. Phys.* **136**, 1 (2004).
15. R. Blaauwgeers, M. Blazkova, M. Clovecko, V.B. Eltsov, R. de Graaf, J. Hosio, M. Krusius, D. Schmoranzer, W. Schoepe, L. Skrbek, P. Skyba, R.E. Solntsev, and D.E. Zmeev, *J. Low Temp. Phys.* **146**, 537 (2007).
16. M. Blažková, M. Človečko, V.B. Eltsov, E. Gažo, R. de Graaf, J.J. Hosio, M. Krusius, D. Schmoranzer, W. Schoepe, L. Skrbek, P. Skyba, R.E. Solntsev, and W.F. Vinen, *J. Low Temp. Phys.* **150**, 525 (2008).
17. G. Sheshin, A.A. Zadorozhko, E. Rudavskii, V. Chagovets, L. Skrbek, and M. Blazhkova, *Fiz. Nizk. Temp.* **34**, 1111 (2008) [*Low Temp. Phys.* **34**, 875 (2008)].
18. D.I. Bradley, M.J. Fear, S.N. Fisher, A.M. Guénault, R.P. Haley, C.R. Lawson, P.V.E. McClintock, G.R. Pickett, R. Schanen, V. Tsepelin, and L.A. Wheatland, *J. Low. Temp. Phys.* **156**, 116 (2009).
19. M. Blazkova, D. Schmoranzer, L. Skrbek, and W.F. Vinen, *Phys. Rev. B* **79**, 054522 (2009).
20. M. Blažková, M. Človečko, E. Gažo, L. Skrbek, and P. Skyba, *J. Low Temp. Phys.* **148**, 305 (2007).
21. V.B. Efimov, D. Garg, O. Kolosov, and P.V.E. McClintock, *J. Low Temp. Phys.* **158**, 456 (2010).

22. D. Schmoranzer and L. Skrbek, *J. Phys.: Conf. Ser*. **150**, 012048 (2009).
23. R. Goto, S. Fujiyama, H. Yano, Y. Nago, N. Hashimoto, K. Obara, O. Ishikawa, M. Tsubota, and T. Hata, *Phys. Rev. Lett*. **100**, 045301 (2008).
24. L. Landau, *J. Phys. USSR* **5**, 71 (1941).
25. L. Landau, *J. Phys. USSR* **11**, 91 (1947).
26. T. Ellis and P.V.E. McClintock, *Philos. Trans. R. Soc. London, Ser. A* **315**, 259 (1985).
27. D. Schmoranzer, M. La Mantia, G. Sheshin, I. Gritsenko, A. Zadorozhko, M. Rotter, and L. Skrbek, *J. Low Temp. Phys*. **163**, 317 (2011).
28. A. Salmela, J. Tuoriniemi, and T. Rysti, *J. Low Temp. Phys*. **162**, 678 (2011).
29. H.A. Nichol, L. Skrbek, P.C. Hendry, and P.V.E. McClintock, *Phys. Rev. E* **70**, 056307 (2004).
30. V.B. Efimov, D. Garg, M. Giltrow, P.V.E. McClintock, L. Skrbek, and W.F. Vinen, *J. Low Temp. Phys*. **158**, 462 (2010).
31. D.I. Bradley, M. Človečko, S.N. Fisher, D. Garg, E. Guise, R.P. Haley, O. Kolosov, G.R. Pickett, V. Tsepelin, D. Schmoranzer, and L. Skrbek, *Phys. Rev. B* **85**, 014501 (2011).